Chaotic motion around prolate deformed bodies

Eduardo Guéron* and Patricio S. Letelier†

Departamento de Matemática Aplicada, Instituto de Matemática, Estatística e Computação Científica, Universidade Estadual de Campinas, 13083-970, Campinas, SP, Brazil

The motion of particles in the field of forces associated to an axially symmetric attraction center modeled by a monopolar term plus a prolate quadrupole deformations is studied using Poincaré surface of sections and Lyapunov characteristic numbers. We find chaotic motion for certain values of the parameters, and that the instability of the orbits increases when the quadrupole parameter increases. A general relativistic analog is briefly discussed.

Attraction forces represented by a monopolar plus a prolate quadrupolar distribution of masses (charges) are a good approximation for elongated massive (charged) bodies. Examples range from astrophysics to nuclear physics. There are many observed galaxy clusters with a cigarlike shape [1]. Also, the nuclear charge of light gold atoms has been reported as having a large prolate deformation [2]. Most of the dwarf galaxies in the virgo cluster may obey the ''prolate hypothesis,'' i.e., they probably have a prolate spheroidal shape [3]. Asteroids also have a prolate shape, but usually they are not axisymmetric. Merrit [4] found, from detailed modeling of triaxial galaxies, that most of the galaxies must be nearly axisymmetric, either prolate or oblate.

Classical, as well as quantum chaos have been studied in a variety of axially symmetric fields of forces. In particular, attraction centers described by potentials that are the sum of two terms: a monopolar term and a quadrupolar deformation. Furthermore, this center is ''perturbed'' by an external distribution of masses (charges) represented by its external multipolar moments, i.e.,

$$V = -\alpha/R - qP_2(\cos\vartheta)/R^2 + V_P, \qquad (1)$$

$$V_P = Q_1 R P_1(\cos\vartheta) + Q_2 R^2 P_2(\cos\vartheta) + \cdots. \qquad (2)$$

Sometimes the monopolar term is changed by the potential of a spring [5]. In general, in all these cases the terms that originate the chaos are the external multipolar moments.

We shall consider the simplest, albeit, important case of a particle moving in the field of a monopole plus a quadrupole deformation. This deformation is usually considered to be the major deviation from spherical symmetry. In cylindrical coordinates, (r,φ,z), the field takes the generic form

$$U(r,z) = -\frac{\alpha}{\sqrt{r^2+z^2}} - \frac{q(2z^2-r^2)}{2(r^2+z^2)^{5/2}}, \qquad (3)$$

where α is a constant that may be associated with the central body mass (charge). It is instructive to have a special model in mind; consider two equal masses located on the z axis

symmetrically, at $z=-a$ and $z=+a$. The gravitational potential of the above mass configuration up to the order a^3 is Eq. (3) with $q=2\alpha a^2$. We shall use $\alpha=1$ without loss of generality. Note that we are not considering external multipolar moments ($V_P=0$), i.e., only deformed cores will be studied.

We can distinguish two cases depending on the sign of q. The first is the oblate deformation case, $q<0$. This is the common case for bodies deformed by rotation and has been analyzed in astronomy for more than 200 years. The integrability of the Newton equations for a particle moving in the gravitational field of an axially symmetric oblate body is an unsolved problem. It is known as the classical problem of the existence of the third isolating integral of motion [6]. There are numerical evidences that orbits of particles moving around a monopole plus an oblate quadrupole are not chaotic. The second case is the prolate deformation case, $q>0$; that is the one that we shall discuss in this Rapid Communication. In this case we have a monopolar field (the usual Kepler problem) ''perturbed'' by a quadrupolar term, in other words, we have a typical situation wherein the Kolmogorov-Arnold-Moser (KAM) theory applies [7].

First we study the contours of the effective potential $U_{eff} = U + h_z^2/(2r^2)$, where $h_z = r^2\dot\varphi$ is the axial specific angular momentum that due to the axial symmetry is conserved. We also have the conservation of the total specific energy, $E = (\dot{r}^2 + \dot{z}^2)/2 + U_{eff}$. Thus, we have that the motion is completely determined by the functions $r=r(t)$ and $z=z(t)$. Then, we have a four-dimensional phase space. But, due to energy conservation the motion actually takes place in a three-dimensional space. An adequate tool to investigate the trajectories in this phase space is the Poincaré surface of section method. Now let us come back to the effective potential contours. In Fig. 1 we plot the level contours of U_{eff} for $L_z = 0.83$ and $E = 0.464$ and different values of the quadrupole moment parameter: (a) $q=0.3$, (b) $q=0.5$, (c) $q=0.85$, and (d) q=0.95. Thus, for these values of the parameters the motion of the particle is confined to toroidal regions that do not contain the symmetry axis. Note that for the last case we have two nonconnected regions.

The particles move in the reduced phase space ($p_r = \dot{r}, r, z$). Note that $p_z = \dot{z}$ is determined by the energy conservation. In Fig. 2, for case (a), we present the intersection

*Email address: gueron@ime.unicamp.br

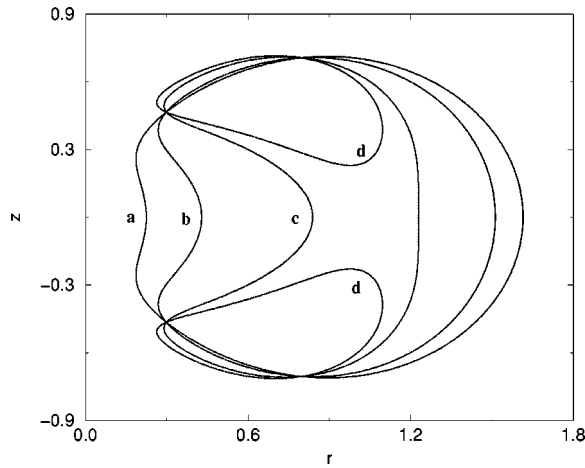†Email address: letelier@ime.unicamp.br

FIG. 1. We plot the level contours of U_{eff} for $L_z = 0.83$ and $E = 0.464$ and different values of the quadrupole moment parameter: (a) $q = 0.3$, (b) $q = 0.5$, (c) $q = 0.85$, and (d) $q = 0.95$.

FIG. 3. Surface of section for $L_z = 0.83$ and $E = 0.464$ and $q = 0.5$. The section corresponds to the plane $z = 0$. For these values of the parameters we have the typical section indicating chaotic motion.

points of some particle trajectories with the plane $z = 0$. The picture is the one for regular orbits. Case (b) is analyzed in Fig. 3, using the same surface section. We find regions of nondestroyed tori together with chaotic regions in concordance with the KAM theory. In Fig. 4 we show again case (b) but, now with a different section, $z = 0.4$. We see that the integrable and chaotic regions are deformed depending on the chosen section. We also studied case (c) that is quite similar to the former, so we shall not present it here. We find that increasing the quadrupole moment the size of the chaotic regions also increases. And finally, in Fig. 5 we study orbits in one of the nonconnected regions of case (d). In this last case the surface section is taken as $z = 0.4$, again we find large regions of chaotic behavior and some nondestroyed tori. In summary, we find chaotic behavior of orbits for several values of prolate quadrupole moment.

To quantify the degree of instability of the orbits we shall study their associated Lyapunov characteristic numbers ($\mathcal{N}$) that are defined as the double limit
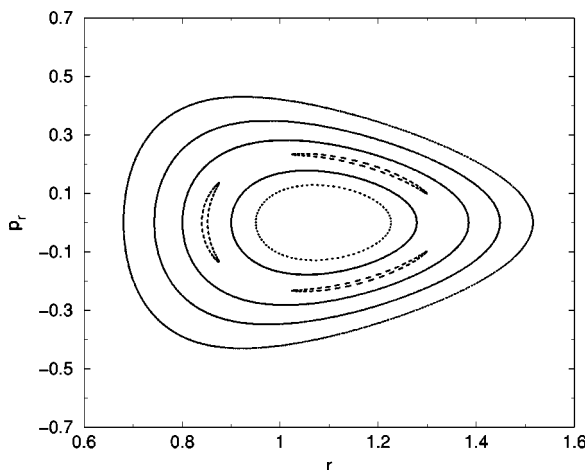
$$\mathcal{N} = \lim_{\substack{\delta_0 \to 0 \\ t \to \infty}} \left[\frac{\log(\delta / \delta_0)}{t} \right], \qquad (4)$$

where δ_0 and δ are the deviation of two nearby orbits at times 0 and t respectively. We get the largest $\mathcal{N}$ by using the technique suggested by Benettin et al. [8]

We fix the value of the constants of motion as $L_z = 0.83$ and $E = 0.464$, and choose the same values of quadrupole parameters used to plot the Poincaré sections. For the value $q = 0.3$ it was chosen the reference orbit with initial conditions: $z = 0$, $p_r = 0$, and $r = 0.85$, and $\delta_0 \simeq 10^{-9}$, we found $\mathcal{N} \lesssim 10^{-4}$ that characterizes a stable system. With $q = 0.5$ and initial conditions: $z = 0$, $p_r = 0.2$. Finally, for $q = 0.95$, and $z = 0.4$, $p_r = 0.05$, and $r = 0.95$, we obtain $\mathcal{N} \simeq 0.09$ (± 0.015). We see that the degree of instability increases when the quadrupole parameter increases for fixed constants of motion.

FIG. 2. Surface of section for $L_z = 0.83$ and $E = 0.464$ and $q = 0.3$. The section corresponds to the plane $z = 0$. For these values of the parameters we have the section of regular motion.
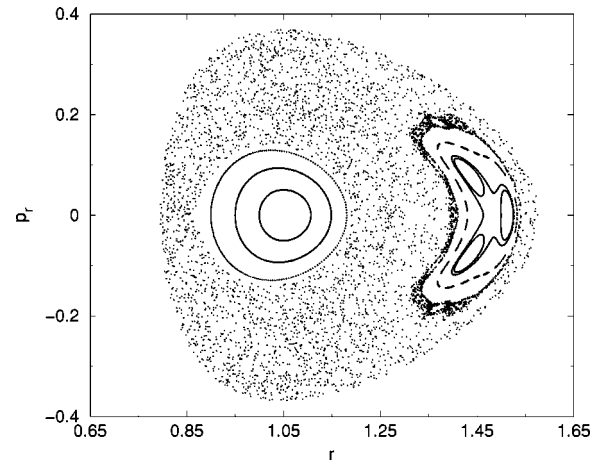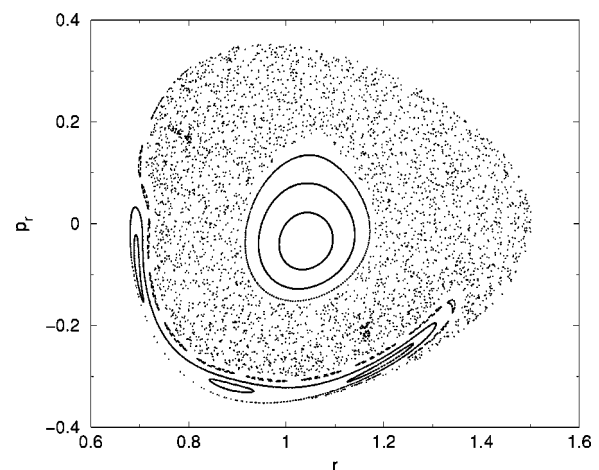

FIG. 4. Surface of section for the same values of the parameters that in the precedent figure, but a different section, $z = 0.4$. We see a different cut of the regular and chaotic regions.
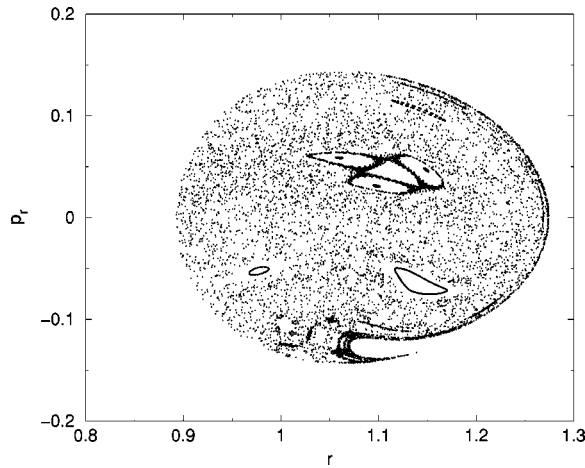
FIG. 5. Surface of section for $L_z = 0.83$ and $E = 0.464$ and $q = 0.95$. The section corresponds to the plane $z = 0.4$. Again we have irregular motion.

As we said before, there are numerical evidences that orbits of particles moving around a monopole plus an oblate quadrupole are not chaotic. The difference between the oblate and the prolate case can be understood by analyzing the critical points of the effective potential U_{eff}. In particular, the existence of the saddle points is one of the main ingredients of instable motion. We find that the critical point, $r = \sqrt{(3q + 2L_z^2)/2\alpha}$, $z = 0$, is a saddle point if the parameters obey the two conditions, $L_z^2 < 3q$ and $3L_z^2 > \sqrt{2\alpha/3}$. Therefore, when $q < 0$, the oblate case, no real L_z can obey the first of these condition.

The Newtonian motion of a particle moving in potential (3) has a general relativistic analogue. The potential is replaced by a metric solution to the vacuum Einstein equation and the particle motion equation by the geodesic equation. The instability of geodesics in metrics associated to a black hole surrounded by a shell of matter was studied in some detail in Ref. [9].
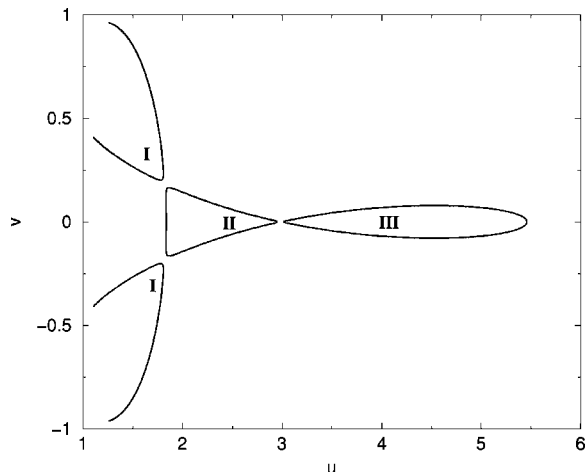

FIG. 6. Level contour for the general relativistic quadrupole + monopole system (ERQ solution). The relativistic constants are $L_z = 3.32$ and $E = 0.937$ and $q = 5.02$. The labels u and v denote spheroidal coordinates.
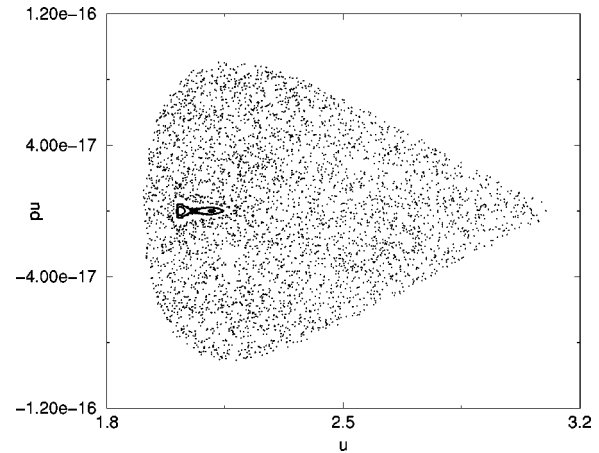

FIG. 7. Surface of section for region II shown in the previous figure. We have a large region of chaotic motion. The section corresponds to the plane $v = 0$, i.e., $z = 0$.

A solution to the Einstein equations that has as a Newtonian limit a potential such as Eq. (3) is the Erez-Rosen-Quevedo (ERQ) solution [10]. We did not find chaos in the oblate case, but the prolate case is chaotic. The confinement region for the relativistic motion constants, $E = 0.937$, and $L_z = 3.322$, and the quadrupole parameter $q = 5.02$ is presented in Fig. 6. The coordinates used in this case are spheroidal coordinates, which are the ones appropriate for the ERQ solution. They are related to the usual cylindrical coordinates by $u = (R_+ + R_-)/(2m)$, and $v = (R_+ - R_-)/(2m)$, with $R_\pm = [r^2 + (z \pm m)^2]^{1/2}$. We have two regions of confinements that we have labeled II and III. In Fig. 7 we present a Poincaré section for particles moving in the region II, the section is taken as $v = 0$, i.e., $z = 0$; u, p_u are canonical conjugate variables. We see a phase space with a large region of chaotic motion. We shall present a complete study of geodesic in ERQ spacetimes elsewhere.

Some dense cores in dark clouds have been found to have prolate spheroidal shape [12]. Then a prolate geometry has to be considered as initial condition in the star formation process. We think that the strong instability presented here may play a crucial effect in the formation of structures in starts [11].

We want to finish this short communication by reminding one that in nonlinear systems of equations chaos is the rule rather than the exception. Thus, simple systems with a minimum of structure play an important role in the physical, as well as, mathematical understanding of chaos. A good example is the paradigmatic Henón-Heiles system wherein the ''simple'' addition of a $x^2 y$ term in the potential of two uncoupled oscillators (integrable motion) has dramatic consequences that are the physical manifestation of the creation of a saddle point together with a perturbation. In the case presented here, we have a similar situation, the prolate-quadrupole potential also adds a saddle and a perturbation.

[1] A.R. Cooray, Mon. Not. R. Astron. Soc. **313**, 783 (2000).

[2] B. Hinfurtner *et al.*, Phys. Rev. Lett. **67**, 812 (1991).

[3] B.S. Ryden, Astrophys. J. **461**, 146 (1996).

[4] D. Merrit, Science **271**, 337 (1996).

[5] See, for instance, W.D. Heiss, R.G. Nazmitdinov, and S. Radu, Phys. Rev. Lett. **72**, 2351 (1995); Phys. Rev. C **52**, 3032 (1995).

[6] See, for instance, D. Baccaletti and G. Pucacco, *Theory of Orbits* (Springer, Berlin, 1998).

[7] See, for instance, J. Guckenheimer and P. Holmes, *Nonlinear Oscillations, Dynamical Systems, and Bifurcation of Vector Fields* (Springer, New York, 1983).

[8] G. Benettin, L. Galgani, and A. Giorgilli, Phys. Rev. A **14**, 2338 (1976).

[9] W.M. Vieira and P.S. Letelier, Astrophys. J. **513**, 383 (1999).

[10] H. Quevedo, Phys. Rev. D **39**, 2904 (1989), and references therein.

[11] Work along this line will be soon reported.

[12] P.C. Myers *et al.*, Astrophys. J **376**, 561 (1991).